Asymmetry of the Bjerknes positive feedback between the two types of El Niño

Fei Zheng[1], Xiang-Hui Fang[1,2], Jin-Yi Yu[3], and Jiang Zhu[1]

[1]International Center for Climate and Environment Science, Institute of Atmospheric Physics, Chinese Academy of Sciences, Beijing, China, [2]College of Earth Science, University of the Chinese Academy of Sciences, Beijing, China, [3]Department of Earth System Science, University of California, Irvine, California, USA

Abstract Corresponding to the pronounced amplitude asymmetry for the central Pacific (CP) and eastern Pacific (EP) types of El Niño, an asymmetry in the strength of the Bjerknes positive feedback is found between these two types of El Niño, which is manifested as a weaker relationship between the zonal wind anomaly and the zonal gradient of sea surface temperature (SST) anomaly in the CP El Niño. The strength asymmetry mainly comes from a weaker sensitivity of the zonal gradient of sea level pressure (SLP) anomaly to that of diabatic heating anomaly during CP El Niño. This weaker sensitivity is caused by (1) a large cancelation induced by the negative SST-cloud thermodynamic feedback to the positive dynamical feedback for CP El Niño, (2) an off-equator shift of the maximum SLP anomalies during CP El Niño, and (3) a suppression of the mean low-level convergence when CP El Niño events occur more often.

1. Introduction

El Niño–Southern Oscillation (ENSO), which is the strongest mode of interannual variability on Earth, has been extensively studied for several decades. Understanding the changes in its characteristics is still an important issue for worldwide environmental and socioeconomic interests [*McPhaden et al.*, 2006; *Ashok and Yamagata*, 2009], especially as a different type of El Niño has been identified recently. Maximum sea surface temperature (SST) anomalies of this type of El Niño are confined mostly in the central Pacific; and therefore, this type has been referred to as the central Pacific (CP) El Niño [*Yu and Kao*, 2007; *Yu et al.*, 2010]. The canonical El Niño has its maximum warming anomalies located in the eastern Pacific and is referred to as the eastern Pacific (EP) El Niño. *Lee and McPhaden* [2010] showed that the intensity of CP El Niño has almost doubled in the past three decades.

Many recent studies have focused on explaining why the CP El Niño has occurred more frequently in recent decades. *Yeh et al.* [2009] suggested that this is likely a consequence of anthropogenically forced global warming. *McPhaden et al.* [2011] pointed out that the background state changes (i.e., a La Niña-like background state with enhanced trade winds and a more tilted thermocline) observed in the tropical Pacific in last decade are opposite from those expected to produce more frequent CP El Niño events. *Xiang et al.* [2012] argued that such state changes in the Pacific may favor the generation of the CP El Niño by suppressing convection and low-level convergence in the central Pacific, which shifts the anomalous convection westward. *Yu et al.* [2012] argued that the atmospheric circulation that dominates the atmosphere-ocean coupling in the tropical Pacific may have changed from the Walker circulation to the Hadley circulation after the 1990s, which allows the CP El Niño to occur more frequently according to the extratropical excitation mechanism they proposed for the CP El Niño.

Besides the difference in their locations, the CP and EP types of El Niño have a pronounced asymmetry in their amplitudes. CP El Niño events tend to be weaker than EP El Niño events. This amplitude asymmetry is also not fully understood. The dominant physical process responsible for the development of El Niño is the so-called Bjerknes feedback [*Bjerknes*, 1969], which describes the sensitivity of the atmospheric response to ocean forcing and vice versa. In this study, a possible asymmetry in the Bjerknes feedback between the two types of El Niño is examined by quantitatively comparing the subprocesses involved in the Bjerknes feedback using data from the past three decades.

2. Data Sets and the Regression Method

Observational and reanalysis data sets were used to analyze the developing phase of El Niño. The wind stress data used were from National Centers for Environmental Prediction (NCEP)-Department of Energy Atmospheric

Model Intercomparison Project-II Reanalysis products [*Kanamitsu et al.,* 2002]; the precipitation data were from the Global Precipitation Climatology Project, v2.2 [*Adler et al.,* 2003]; and the SST data were from the extended reconstructed SST (NOAA), v3b [*Smith et al.,* 2008]. The analysis period of the above data sets is from 1980 to 2010. A slightly shorter period from 1984 to 2009 is used for the cloud amount data from the International Satellite Cloud Climatology Project, D2 [*Rossow and Schiffer,* 1999], and for the net surface downward full-sky shortwave radiation flux data from objectively analyzed air-sea fluxes [*Yu and Weller,* 2007].

Following *Xiang et al.* [2012], five events were chosen for the CP El Niño (1991/1992, 1994/1995, 2002/2003, 2004/2005, and 2009/2010) and four events for the EP El Niño (1982/1983, 1986/1987, 1997/1998, and 2006/2007). For each event, the developing phase was defined as from the month when the oceanic Niño index becomes larger than 0.5℃ to the end of the calendar year. For example, the developing phase was from May to December for the 1982/1983 El Niño event and from August to December for the 1986/1987 El Niño event.

In this study, the Bjerknes feedback is quantified by the regression coefficients between pairs of variables involved in the feedback processes. Since only a limited number of events are available in the observations for both the EP and CP types of El Niño, we choose to use a "robustness regression" method [*Holland and Welsch,* 1977] for the calculation of the regression coefficients. Robust regression method is a form of regression analysis designed to be not overly affected by violations of assumptions by the underlying data-generating process, and thus is considered less sensitive than the ordinary least squares regression method to large changes in small parts of the data [*Rousseeuw and Leroy,* 1987], meaning the regression coefficients determined with this method are influenced less by outliers.

3. Differences in the Strength of the Bjerknes Positive Feedback

Bjerknes [1969] pointed out that an initial positive SST anomaly in the equatorial eastern Pacific reduces the east-west SST gradient and hence weakens the Walker circulation, which results in weaker trade winds over the tropical Pacific. The weaker trade winds further drive oceanic processes to reinforce the SST anomaly. The strength of this Bjerknes positive feedback can, therefore, be measured as the correlation or regression between zonal gradient of SST anomaly (dSST/dx) and zonal wind stress (τ_x), namely dSST/dx $\rightarrow \tau_x$. Three subprocesses are involved in this Bjerknes positive feedback. First, the east-west gradient of the SST anomalies leads to an east-west gradient in total diabatic heating (Q) through atmospheric convection, precipitation, clouds, water vapor, etc. (dSST/dx $\rightarrow dQ$/dx). The diabatic heating is composed of the latent heating from precipitation and the solar radiative heating related to clouds and water vapor. Very often the diabatic heating is represented only by the latent heating related to the precipitation (dQ/dx $\approx d$Prec/dx), due to lack of cloud data or an assumption that the contribution from the cloud radiative heating is small [*Lin,* 2007]. Thus, the zonal gradient in precipitation is used to characterize the east-west asymmetry in the diabatic heating. The zonal gradient in the diabatic heating results in different variations in sea level pressure (SLP) across the equatorial Pacific (dQ/dx $\rightarrow d$SLP/dx). The pressure gradient further drives τ_x anomalies in the central Pacific (dSLP/dx $\rightarrow \tau_x$). The τ_x in turn enhances the zonal SST anomaly gradient ($\tau_x \rightarrow d$SST/dx) by inducing downwelling/upwelling waves, zonal advection, vertical upwelling/downwelling, and meridional Sverdrup transport. Thus, the primary subprocesses at work in the Bjerknes positive feedback can be illustrated in the following:

$$\frac{dSST}{dx} \rightarrow \frac{dQ}{dx} \approx \frac{dPrec}{dx} \rightarrow \frac{dSLP}{dx} \rightarrow \tau_x$$

We then contrasted each of these three subprocesses in the two types of El Niño using the five CP El Niño and four EP El Niño events. Figure 1 shows the composited anomaly fields during the developing phase of the two types of El Niño. The most noticeable feature in the composites is that the positive SST anomalies during the CP El Niño are situated in the central Pacific and have smaller amplitude than those of the EP El Niño that are located in the eastern Pacific. The zonal distributions of the equatorial (5°S–5°N) SST anomalies for these two types of El Niño are compared in Figure 1 (right column). The center of SST anomaly shifts westward by 43.77° from the EP to CP El Niño. Corresponding to these SST features, the anomalous τ_x, SLP, and precipitation fields associated with the CP El Niño all show smaller amplitudes and similar westward shifts of their structures compared to those of the EP El Niño (statistically significant at the 95% using an *F* test). The similar shifts reflect
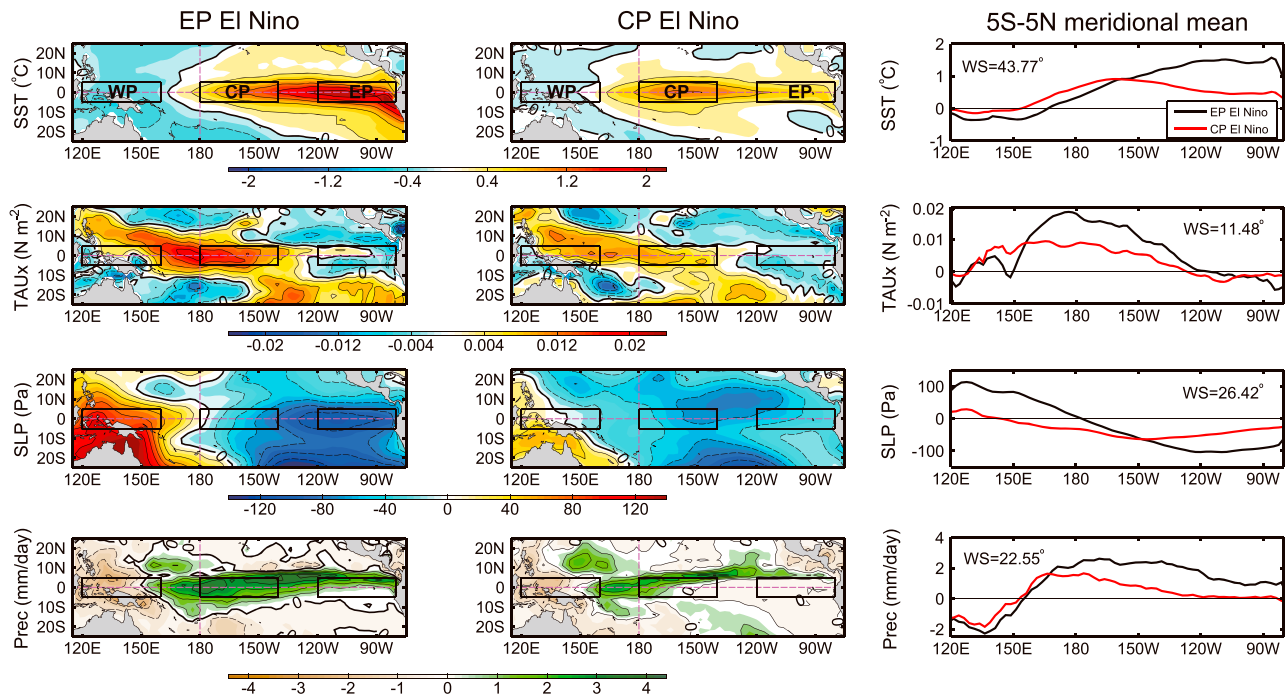
Figure 1. Composites of anomalous SST, τ_x, SLP, and precipitation for the developing phase of (left column) EP El Niño and (middle column) CP El Niño. Contour intervals are 0.4°C, 0.004 N m^{-2}, 20 Pa, and 0.8 mm d^{-1} for anomalous SST, τ_x, SLP, and precipitation, respectively. (right column) The zonal structure for the composite EP El Niño (black lines) and CP El Niño (red lines) averaged over 5°S to 5°N, with the westward shift (WS) of the center of the anomalies from EP El Niño to CP Niño. The WS of these four variables are all significant under the 95% confidence level from an *F* test.

the strong coupling nature between the atmosphere and ocean over the equatorial regions. Another important feature in Figure 1 is that the centers of the SLP anomalies are located over the western and eastern equatorial Pacific during the EP El Niño, but the eastern center during the CP El Niño moves off-equator as reported by *Yu et al.* [2010] using a different analysis method and a different data period.

As mentioned, the composites indicate smaller amplitude for the CP El Niño than for the EP El Niño. We first examined how this amplitude difference can be related to the strength of the Bjerknes positive feedback using the composite shown in Figure 1. In this analysis, all the values involved in the calculation of (1) are first averaged to have a reduced resolution of 10° in longitude and are then averaged between 5°S and 5°N. We defined three boxes in the equatorial Pacific to calculate the cross-basin gradients, primarily based on the SST anomaly patterns. These three boxes are located over the western, central, and eastern regions of the equatorial Pacific and are termed the WP, CP, and EP boxes, respectively (see Figure 1). The EP box covers the region (120°–80°W; 5°S–5°N) where the maximum SST anomalies are located during the developing phase of the EP El Niño. The CP box covers the region (180–140°W; 5°S–5°N), where the maximum SST anomalies are located during the CP El Niño. The WP box is located in the region (120°–160°E; 5°S–5°N), where the minimum (i.e., negative) SST anomalies are located during both types of El Niño. The locations of these boxes are consistent with those selected in *Yu et al.* [2010] for an ocean heat budget analysis of the two types of El Niño. The zonal gradient of SST, SLP, and precipitation were calculated using the EP and WP Boxes for the EP El Niño and using the CP and WP boxes for the CP El Niño. As revealed in Figure 1, there are some phase shifts between the centers of SST anomalies and those of SLP, τ_x, and precipitation anomalies. Nevertheless, the EP, CP, and WP selected based on the locations of the maximum SST anomalies capture large parts of the largest anomalies in the other three variables.

We examined the strength of the Bjerknes feedback by finding the robust regression of τ_x on the zonal SST anomaly gradient along the equatorial Pacific. As shown in Figure 2a, the feedback (i.e., the maximum regression coefficient) is 1.8 times stronger during the EP El Niño than during the CP El Niño. This ratio is consistent with the ratio of the maximum SST anomaly amplitudes shown in Figure 1 between the two types of the El Niño (i.e., 2.32°C for the EP El Niño and 1.24°C for the CP El Niño). The amplitude asymmetry between the two types of El Niño can be explained by the asymmetry in the strengths of their associated Bjerknes feedback. We then examined the first subprocess of the Bjerknes feedback, namely the SLP-to-wind stress
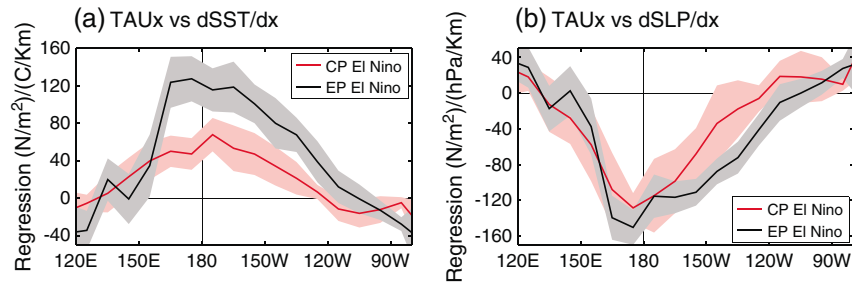
Figure 2. Robust regression coefficients and the corresponding error bars (shaded, 95% confidence for a Student's *t* test) between (a) τ_x and zonal SST gradient and (b) τ_x and zonal SLP gradient during CP (red) and EP (black) El Niño. At each point (10° interval in longitude), the regression coefficient for the EP/CP El Niño is estimated from all monthly anomaly values of τ_x at the point and the calculated dSST/dx. Coefficients between EP and CP El Niños are significantly different where their corresponding error bars are not overlapped, and vice versa.

(dSLP/dx → τ_x) sensitivity, by calculating the robust regression of τ_x on zonal SLP anomaly gradient. It is expected to find from Figure 2b that there is nearly no significant difference between the two types in the maximum value of the regression, meaning the two types produce similar sensitivity of τ_x to zonal SLP gradient variations. Moreover, the results quantified in Figure 2 are not significantly sensitive to the wind stress data set adopted here. We repeated the analyses with wind stress from four other reanalysis data sets (i.e., NCEP1, Operational Ocean Analysis/Reanalysis System (ORA-S3) at ECMWF, Simple Ocean Data Assimilation (SODA), and Wave and Anemometer-Based Sea Surface Wind (WASWinds)) and obtained similar results. This also confirms the conclusion drawn in *McGregor et al.* [2012] that the choice of wind stress product is relatively unimportant if the focus is only on high-frequency (i.e., interannual) variability. Therefore, the reason for the striking difference in the strength of the Bjerknes feedback must be in the other two subprocesses of (1) that link SST to SLP through diabatic heating: the SST-to-precipitation sensitivity (dSST/dx → dPrec/dx) and the Precipitation-to-SLP sensitivity (dPrec/dx → dSLP/dx).

These two subprocesses link zonal gradients of SST, SLP, and precipitation anomalies across the equatorial Pacific. The monthly anomaly values of the gradients calculated from the developing phases of the four EP El Niño events (black circles) and the five CP El Niño events (red asterisks) are shown in Figure 3a for dSST/dx and dPrec/dx. This figure is used to examine the SST-to-precipitation (dSST/dx → dPrec/dx) sensitivity in the Bjerknes feedback. As indicated by the robust fitting lines in Figure 3a, there is no significant difference between the two types of El Niño in terms of the relationship between the zonal gradients of precipitation and SST anomalies. We next examined the precipitation-to-SLP (dPrec/dx → dSLP/dx) sensitivity in the Bjerknes feedback in Figure 3b. This figure shows that the relations between the SLP and precipitation (which represents the diabatic heating) are very different between the two types of El Niño. First, the zonal gradient of SLP anomaly during the CP El Niño events concentrated mostly in the low-value region (i.e., near the zero line), while they are more uniformly spread across a wide range of gradient values during the EP El Niño events. The small SLP gradients across the equatorial Pacific during the CP El Niño reflect the fact that the
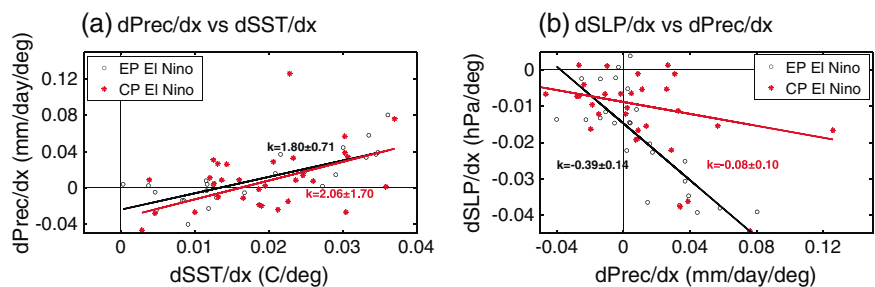

Figure 3. Scatter diagram and the corresponding robust fitting lines (with the values of slopes plus and minus 1.96 standard errors, namely 95% confidence for a Student's *t* test) between (a) zonal precipitation gradient and zonal SST gradient and (b) zonal SLP gradient and zonal precipitation gradient during the CP (red asterisks/lines) and EP (black circles/lines) El Niño. The results are obtained from all monthly anomaly values during the developing phase of the EP and CP El Niños, respectively.

negative SLP anomaly center for these events is off the equator (see Figure 1). Second, in response to a given value of precipitation anomaly gradient, the SLP anomaly gradient is larger for the EP El Niño (i.e., a slope of -0.39 ± 0.14 (hPa/deg)/(mm/day/deg)) than for the CP El Niño (i.e., a slope of -0.08 ± 0.10 (hPa/deg)/(mm/day/deg)). This difference indicates that the same value of the zonal precipitation heating gradient along the equatorial Pacific tends to induce a larger zonal SLP gradient for the EP El Niño than for the CP El Niño. Therefore, the weaker Bjerknes feedback for the CP El Niño is related to this weaker response of SLP gradient (and thus wind stress) to the precipitation heating gradient induced by the El Niño SST.

Why then is the SLP response to the precipitation heating weaker in the CP El Niño? An interesting feature in Figure 3b offers a clue. It can be seen that the scattering points of (dSLP/dx, dPrec/dx) during the CP El Niño are not as tightly centralizing around the linear fit line as during the EP El Niño. This suggests that the SLP anomaly gradient is more robustly correlated with the heating gradient produced by the latent heat release of precipitation during the EP El Niño events than during the CP El Niño events. There are three possible explanations for this difference. One is from *Yu et al.* [2010], who argued that the CP El Niño induces more variations in the local Hadley circulation than in the Walker circulation, which can result in a weaker zonal SLP anomaly gradient along the equator than during EP El Niño events. The other explanation is from *Xiang et al.* [2012], who argued that the Pacific mean state shifted around the late 1990s toward a La Niña-like pattern, and the suppressed low-level convergence associated with this state over the central Pacific could limit the decrement of the local SLP during the CP El Niño. The third possibility is that there are processes other than the precipitation that also contribute to the total diabatic heating to determine the SLP response. One such possible candidate is the radiative heating associated with clouds, and water vapor that has been neglected in (1), when the total diabatic heating was assumed to be represented by the latent heating alone. It is possible that the cloud radiative heating can be neglected for the EP El Niño but not for the CP El Niño. When the negative diabatic heating anomalies (i.e., $Q < 0$) associated with cloud radiative fluxes increase its importance during CP El Niño events, the negative thermodynamic feedback produced by the cloud radiative effect may cancel out the positive diabatic heating anomalies associated with precipitation anomalies. As a result of this possible cancelation, the SLP anomalies induced by the total diabatic heating during the CP El Niño maybe not as large as during the EP El Niño. The smaller SLP anomalies then force weaker westerly wind stress anomalies along the equator and result in a weaker Bjerknes feedback.

To examine the above hypothesis concerning the cloud radiative effect, we examined the total cloud amount and shortwave flux anomaly composites for the two types of El Niño. The composites were constructed from the three EP El Niño events (1986/1987, 1997/1998, and 2006/2007) and the five CP El Niño events (1991/1992, 1994/1995, 2002/2003, 2004/2005, and 2009/2010) that occurred during the period when data were available (1984–2009). Figure 4 shows that during the both types of El Niño, the centers of positive cloud amount anomalies are located in the central Pacific. The increased total cloud amounts decrease the net surface solar radiation heating into the ocean, which is shown in Figure 4 (bottom row). The decreased shortwave flux results in diabatic cooling anomalies in the central Pacific. Since CP El Niño events have their maximum diabatic heating anomalies induced by precipitation in the central Pacific (see Figure 4 (top row) where the composite precipitation anomalies are shown), these precipitation heating anomalies are greatly canceled out by the cloud radiation cooling anomalies. However, during the EP El Niño events, the precipitation heating anomalies occur over a zonal band extending from eastern Pacific to central Pacific and are not largely canceled out by the cloud radiating cooling anomalies in the central Pacific. As a result, the sensitivity of the zonal SLP gradient to the zonal precipitation anomalies is larger for the EP El Niño than for the CP El Niño, as revealed in Figure 3b. This explains the strong linear correlation between the zonal SLP anomaly gradient and the zonal precipitation anomaly gradient in Figure 3b. Therefore, Figure 4 demonstrates that the different importance of the cloud radiative effects is a cause for the different strengths of the Bjerknes feedback found during the EP and CP types of El Niño.

It is noted that the 1990/91 El Niño event coincided with the Pinatubo volcano eruption. The composite results shown for the CP El Niño (Figures 2–4) can be impacted by the volcanic effects. To examine this possible impact, we repeated the analyses for these figures without the 1990/1991 event and found similar results (not shown). It is likely due to the fact that our analyses focus on the onset to growing periods of El Niño event, while the Pinatubo eruption is known to impact the decaying phase of the 1990/1991 El Niño event [e.g., *Graf and Zanchettin*, 2012].
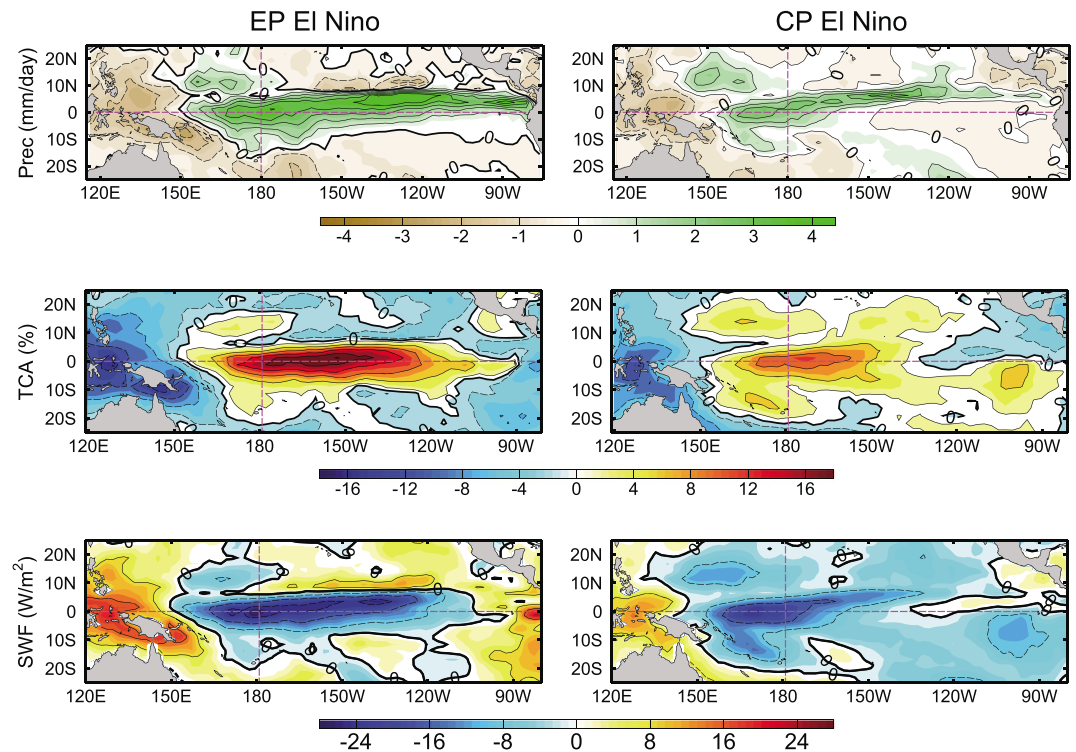
Figure 4. Composites of anomalous precipitation ((top row) contour interval is 0.8 mm/d), total cloud amount ((middle row) contour interval is 4%), and net surface downward full-sky shortwave radiation flux ((bottom row) contour interval is 8 W/m^2) for the developing phase of EP (left column) and CP (right column) El Niño.

4. Discussion and Conclusions

In this work, the strong asymmetry between the amplitudes of the EP and CP El Niño is studied by analyzing the three subprocesses of the Bjerknes positive feedback. The results show that the asymmetry in the strength of the Bjerknes positive feedback is mainly caused by the different relationships between the zonal SLP anomaly gradient and the zonal precipitation anomaly gradient during the developing phase of the two types of El Niño. The different relationships are explained by three reasons. The first of them is the eastern center of SLP anomalies during the CP El Niño moves from the equatorial Pacific to the off-equatorial Pacific, which is related to the shift of the governing atmospheric circulation during the two type of El Niño as suggested in *Yu et al.* [2010]. The second reason is related to a shift of the Pacific mean state toward a La Niña-like pattern in the recent decade, which tends to suppress the low-level convergence over the central Pacific and limit the low range of local SLP [*Xiang et al.,* 2012]. The third reason that we emphasized here is the effect produced by the cloud radiative process during the El Niño. Cloud amounts are found to increase over the central Pacific during both types of El Niño, which coincide with the location of the maximum precipitation heating anomalies during the CP El Niño but not during the EP El Niño. Therefore, the cooling produced by the cloud radiative effect does not limit the development of the EP El Niño as much as it does for the CP El Niño. In other words, the negative thermodynamic feedback produced by the cloud radiative effect largely weakens the positive dynamical feedback represented in (1) for the CP El Niño but nor for the EP El Niño.

By analyzing the subprocesses involved in the Bjerknes positive feedback, this study identifies the cloud radiative process as one key factor in causing the amplitude asymmetry between the CP and EP El Niño. It should be noted that the results reported here can only be considered as suggestive due to the limited number of available EP and CP El Niño events used in the analyses. Further studies are needed to fully understand the role of precipitation, cloud, and radiative processes in causing the ENSO diversity. On the other hand, other processes, such as the fresh water flux and its related salinity variations, may be other factors in modulating the SST over the central Pacific, as mentioned in *Zheng and Zhang* [2012].

References

Adler, R. F., et al. (2003), The version-2 Global Precipitation Climatology Project (GPCP) monthly precipitation analysis (1979-present), *J. Hydrometeor.*, *4*, 1147–1167.

Ashok, K., and T. Yamagata (2009), Climate change: The El Niño with a difference, *Nature*, *461*, 481–484, doi:10.1038/461481a.

Bjerknes, J. (1969), Atmospheric teleconnections from the equatorial Pacific, *Mon. Weather Rev.*, *97*, 163–172.

Graf, H.-F., and D. Zanchettin (2012), Central Pacific El Niño, the "subtropical bridge," and Eurasian climate, *J. Geophys. Res.*, *117*, D01102, doi:10.1029/2011JD016493.

Holland, P. W., and R. E. Welsch (1977), Robust regression using iteratively reweighted least-squares, *Commun. Stat. Theor. Methods*, *A6*, 813–827.

Kanamitsu, M., W. Ebisuzaki, J. Woollen, S. Yang, J. J. Hnilo, M. Fiorino, and G. L. Potter (2002), NCEP-DEO AMIP-II Reanalysis (R-2), *Bull. Am. Meteorol. Soc.*, *83*, 1631–1643, doi:10.1175/BAMS-83-11-1631.

Lee, T., and M. J. McPhaden (2010), Increasing intensity of El Niño in the central-equatorial Pacific, *Geophys. Res. Lett.*, *37*, L14603, doi:10.1029/2010GL044007.

Lin, J.-L. (2007), The double-ITCZ Problem in IPCC AR4 coupled GCMs: Ocean-atmosphere feedback analysis, *J. Climate*, *20*, 4497–4525, doi:10.1175/jcli4272.1.

McGregor, S., A. Sen Gupta, and M. H. England (2012), Constraining wind stress products with sea surface height observations and implications for Pacific Ocean sea level trend attribution, *J. Climate*, *25*, 8164–8176.

McPhaden, M. J., S. E. Zebiak, and M. H. Glantz (2006), ENSO as an integrating concept in Earth science, *Science*, *314*, 1739–1745.

McPhaden, M. J., T. Lee, and D. McClurg (2011), El Niño and its relationship to changing background conditions in the tropical Pacific Ocean, *Geophys. Res. Lett.*, *38*, L15709, doi:10.1029/2011GL048275.

Rossow, W. B., and R. A. Schiffer (1999), Advances in understanding clouds from ISCCP, *Bull. Am. Meteorol. Soc.*, *80*, 2261–2287.

Rousseeuw, R. J., and A. M. Leroy (1987), *Robust Regression and Outlier Detection*, John Wiley, New York.

Smith, T. M., R. W. Reynolds, T. C. Peterson, and J. Lawrimore (2008), Improvements to NOAA's historical merged land-ocean surface temperature analysis (1880–2006), *J. Climate*, *21*, 2283–2296, doi:10.1175/2007JCLI2100.1.

Xiang, B.-Q., B. Wang, and T. Li (2012), A new paradigm for the predominance of standing Central Pacific Warming after the late 1990s, *Clim. Dyn.*, doi:10.1007/s00382-012-1427-8.

Yeh, S.-W., J.-S. Kug, B. Dewitte, M.-H. Kwon, B. P. Kirtman, and F.-F. Jin (2009), El Niño in a changing climate, *Nature*, *461*, 511–514, doi:10.1038/nature08316.

Yu, J.-Y., and H.-Y. Kao (2007), Decadal changes of ENSO persistence barrier in SST and ocean heat content indices: 1958–2001, *J. Geophys. Res.*, *112*, D13106, doi:10.1029/2006JD007654.

Yu, J.-Y., H.-Y. Kao, and T. Lee (2010), Subtropics-related interannual sea surface temperature variability in the equatorial central Pacific, *J. Climate*, *23*, 2869–2884, doi:10.1175/2010JCLI3171.1.

Yu, J.-Y., Y.-H. Zou, S.-T. Kim, and T. Lee (2012), The changing impact of El Niño on US winter temperatures, *Geophys. Res. Lett.*, *39*, L15702, doi:10.1029/2012GL052483.

Yu, L., and R. A. Weller (2007), Objectively analyzed air-sea heat fluxes for the global ice-free oceans (1981–2005), *Bull. Am. Meteorol. Soc.*, *88*, 527–539.

Zheng, F., and R.-H. Zhang (2012), Effects of interannual salinity variability and freshwater flux forcing on the development of the 2007/08 La Niña event diagnosed from Argo and satellite data, *Dyn. Atmos. Oceans.*, *57*, 45–57.